

# UC San Diego

## UC San Diego Electronic Theses and Dissertations

### Title

Establishing CellROX Deep Red as a Radical Dosimeter for Fast Photochemical Oxidation of Proteins (FPOP)

### Permalink

<https://escholarship.org/uc/item/6sk2x4sv>

### Author

Ross, Imani Lillian

### Publication Date

2024

Peer reviewed|Thesis/dissertation

UNIVERSITY OF CALIFORNIA SAN DIEGO

Establishing CellROX Deep Red as a Radical Dosimeter for Fast Photochemical Oxidation of  
Proteins (FPOP)

A Thesis submitted in partial satisfaction of the requirements  
for the degree Master of Science

in

Chemistry

by

Imani Lillian Ross

Committee in charge:

Professor Lisa Jones, Chair  
Professor Elizabeth Komives  
Professor Brian Leigh

2024

Copyright

Imani Lillian Ross, 2024

All rights reserved.

The Thesis of Imani Lillian Ross is approved, and it is acceptable in quality and form for publication on microfilm and electronically.

University of California San Diego

2024

## DEDICATION

I dedicate this thesis to my family as well as to my friend who recently passed away.

Mom, Dad, Logan, Tomi, this is for you.

## TABLE OF CONTENTS

THESIS APPROVAL PAGE .....	iii
DEDICATION .....	iv
TABLE OF CONTENTS .....	v
LIST OF FIGURES .....	vi
LIST OF TABLES .....	vii
LIST OF ABBREVIATIONS .....	viii
ACKNOWLEDGEMENTS .....	ix
VITA .....	x
ABSTRACT OF THE THESIS .....	xi
Chapter 1 Incorporating Dosimetry into an IC-FPOP Workflow .....	1
Chapter 2 Troubleshooting and Optimization of Fluorescence Imaging .....	8
CONCLUSION .....	14
REFERENCES .....	16

## LIST OF FIGURES

Figure 1: PIXY 2.0.....	4
Figure 2: LabVIEW PIXY Benchmark script for a six-well plate.....	5
Figure 3: IC-FPOP Workflow.....	6
Figure 4: Dose response curve of CellROX Deep Red in laser samples at different concentrations of hydrogen peroxide (0, 20, 40, 80, and 100 mM).....	7
Figure 5: ImageJ Set Measurements. ....	9
Figure 6: Manual Thresholding in ImageJ.....	10
Figure 7: LabVIEW 24-well automated script.....	11
Figure 8: Dose response curve of CellROX Deep Red in laser samples at different concentrations of hydrogen peroxide (0, 20, 40, 80, and 100 mM) after manual thresholding in ImageJ. ....	12
Figure 9: Dose response curve of CellROX Deep Red in 24-well plate laser samples at different concentrations of hydrogen peroxide (0, 20, 40, 80, and 100 mM) after manual thresholding in ImageJ. ....	12

## LIST OF TABLES

Table 1: Experimental outline with predicted outcomes. A) [H <sub>2</sub> O <sub>2</sub> ] gradient: B) Laser Energy gradient: C) DMSO gradient:.....	15
---	----



## LIST OF ABBREVIATIONS

IC	In-cell
FPOP	Fast Photochemical Oxidation of Proteins
HRPF	Hydroxyl radical protein footprinting
Cy5	Cyanine 5
PIXY	Platform Incubator with movable XY stage
ROS	Reactive oxidative species
H <sub>2</sub> O <sub>2</sub>	Hydrogen peroxide
HEK	Human embryonic kidney
DMEM	Dulbecco's Modified Eagle Medium
FBS	Fetal Bovine Serum
P/S	streptomycin-penicillin
PBN	N-tert-Butyl- $\alpha$ -phenylnitron
DMTU	Dimethylthiourea
DMSO	Dimethyl sulfoxide
PBS	Phosphate-Buffered Saline
SP	Sample protection
TRANS	Transmitted Light
au	arbitrary units

## ACKNOWLEDGEMENTS

This research was conducted in the lab of Professor Lisa M. Jones. I would like to acknowledge Professor Lisa M. Jones for her role as chair of my committee and for her guidance during my time in her lab.

I would like to thank Raquel Shortt for her dedicated training of me along with five other first year graduate students admitted into the Jones Lab. Despite having to relocate and working on her dissertation, she still found time to give us the scientific knowledge needed to begin our graduate school careers.

Much appreciation goes to all of my friends and family, local, east coast, and abroad, that provided the support, insight, and love that has brought me this far. I wouldn't be here without you, and you have made a difficult time manageable.

To my lab mates, Jalah, Haolin, Jorge, Kez, and Luis, thank you for keeping me well-fed and being a joy to be around.

Special thanks to the American Chemical Society (ACS) Bridge Program as funded by Genentech and the National Science Foundation in partnership with the ACS for providing funding, support, and an amazing cohort and group of friends (Kez, Noura, and Luis) with which to pursue my masters. I'd also like to shoutout our senior ACS Bridge cohorts and the fun and counsel they provided. Finally, I'd like to thank Professor Brian Leigh, the University of California, San Diego (UCSD) ACS Director for his advice and service on my committee, Professor Haim Weizman for our talks and his uplifting demeanor, and Professor Elizabeth Komives for her guidance, service on my committee, and understanding.

(Also, thanks to my therapist. Therapy has made all the difference.)

## VITA

- 2022 Bachelor of Science in Chemistry, Howard University
- 2024 Master of Science in Chemistry, University of California San Diego

## PUBLICATIONS

Ross, I. L., Beardslee, J. A., Steil, M. M., Chihanga, T., & Kennedy, M. A. (2023). Statistical considerations and database limitations in NMR-based metabolic profiling studies. *Metabolomics : Official journal of the Metabolomic Society*, 19(7), 64. <https://doi.org/10.1007/s11306-023-02027-5>

## FIELD OF STUDY

Major Field: Chemistry and Biochemistry  
Studies in Biochemistry  
Professor Lisa M. Jones

## ABSTRACT OF THE THESIS

Establishing CellROX Deep Red as a Radical Dosimeter for Fast Photochemical Oxidation of Proteins (FPOP)

by

Imani Lillian Ross

Master of Science in Chemistry

University of California San Diego, 2024

Professor Lisa M. Jones, Chair

Hydroxyl radical protein footprinting (HRPF) coupled to mass spectrometry (MS) is a vital technique in determining the higher order structure of proteins. This method uses hydroxyl radicals to oxidatively modify solvent-accessible amino acids and has recently been extended to in-cell analysis.<sup>4</sup> Specifically, HRPF via in-cell fast photochemical oxidation of proteins (IC-

FPOP) is a relatively new approach to labelling proteins, with the ability to modify 19 of the 20 amino acids. FPOP uses an excimer laser to split hydrogen peroxide ( $H_2O_2$ ) into hydroxyl radicals, which are then able to react with, and thus label solvent-accessible surface residues of a protein on the microsecond time scale. In Lisa Jones's lab, in-cell protein footprinting has been coupled with mass spectrometry to discern protein structure in-cell. Specifically, IC-FPOP has been implemented in a Platform Incubator with a movable XY stage (PIXY)<sup>3</sup> and used to successfully modify proteins in several commonly used cell lines.<sup>4</sup> However, there remains a gap in the IC-FPOP methodology pertaining to the effective radical dose delivered to the cellular environments. While IC-FPOP is an effective avenue of HRPF, a challenge that remains is maintaining reproducibility as it pertains to the concentration of radical that is delivered to the system, or the effective radical dose, of hydroxyl radicals reacting with the protein. Effective radical dose is affected by the amount of radical delivered as well as the presence of other substances, such as radical scavengers. While dosimetry experiments for HRPF via FPOP have been done before in other labs, there is currently no protocol for dosimetry for IC-FPOP. CellROX Deep Red is a fluorescent probe that fluoresces only in the presence of reactive oxidative species (ROS). I propose probing the efficacy of the fluorophore CellROX Deep Red as a radical dosimeter for IC-FPOP. I will first troubleshoot and optimize the fluorescence imaging of HEK293 cells with CellROX Deep Red directly following their oxidation. I will then conduct imaging of the cells having been exposed to increasing values of hydrogen peroxide concentrations in order to demonstrate a linear response of the dosimeter CellROX Deep Red.

## Chapter 1 Incorporating Dosimetry into an IC-FPOP Workflow

Hydroxyl radical protein footprinting (HRPF) by fast photochemical oxidation of proteins (FPOP) is a labeling technique that provides structural information by modifying solvent accessible amino acids. It has been pivotal in studying the higher order structure of proteins. IC-FPOP is a growing technique being used in mass spectrometry-based proteomics that enables the examination of protein conformations within an intricate cellular environment.

A dosimeter enables the accurate measurement of the radical dose delivered to the cell, increasing reproducible and reliable results. The Joshua Sharp group at the University of Mississippi has developed adenine as a radical dosimeter for in-vitro FPOP. Adenine absorbance decreases as it is oxidized.<sup>5</sup> The Sharp group has successfully used dosimetry to perform compensated FPOP where radical scavenging is accounted for and compensated for using dosimetry.<sup>8</sup> However, adenine would not be an appropriate dosimeter for IC-FPOP owing to both the endogenous levels of this molecule in cells and the difficulty in monitoring a loss of signal in a complex sample.

HRPF techniques are limited by their ability to deliver a defined concentration of hydroxyl radicals to the protein. This ability is impacted by both the amount of radical generated and the presence of radical scavengers in solution. In order to compare HRPF data from sample to sample, a hydroxyl radical dosimeter is needed that can measure the effective concentration of radical that is delivered to the protein, after accounting for both differences in hydroxyl radical generation and nonanalyte radical consumption.<sup>7</sup>

CellROX Deep Red is a radical dosimeter that has an emission of 644 to 665nm (Cy5 was used for fluorescence imaging, as its wavelength ranges from 649 to 669 nm). It fluoresces only in the presence of ROS when it becomes oxidized. The Jones lab has previously used this

fluorophore to demonstrate that cells were intact after the completion of IC-FPOP.<sup>2</sup> CellROX Deep Red localized in the cytoplasm, leaving the nucleus intact. This work demonstrated the potential of using CellROX Deep Red as a dosimeter for IC-FPOP.

Human embryonic kidney 293 (HEK293) cells were used for the purposes of IC-FPOP experimentation. In addition to its ease of growth in serum-free suspension culture and its amenability to transfection, this cell line's most important attribute is its human origin, which makes it suitable to produce biologics intended for human use.<sup>1</sup> Human embryonic kidney (HEK) cell lines provide systems that exhibit wide versatility.<sup>6</sup>

### **IC-FPOP Sample Preparation**

To make a collagen solution, 1.06 mL of 3.6 mg/mL collagen was added to 98.94 mL (19 µg/mL) of cell culture water to make a 100 mL. To a six-well plate, 2 mL of the collagen solution was added to each well, coating them in 6-10 µg/cm<sup>2</sup>. The protein was allowed to bind to the plate overnight at 4°C. The next day, excess fluid was removed from the coated surface, and the plate was returned to 4°C and allowed to dry overnight. The coated surfaces were sterilized the next day with three UV cycles of exposure to UV light in a sterile tissue culture hood.

In one T175 flask, HEK293 cells were grown to 80% confluency. One T175 was used to prepare three collagen-coated plates. Collagen plates were rinsed with tissue culture water. The HEK293 cells were rinsed with 7mL of PBS and detached from the bottom of the flask with 2mL of trypsin. The trypsin was neutralized in 10 mL of DMEM media supplemented with FBS and streptomycin-penicillin (P/S). The media was removed, the cells were resuspended in 23 mL of the media, and 1 mL of the cell suspension was added to each well. An additional 3 mL of media

was added to each well. The well plates were placed in a 37°C incubator until cells reached 80% confluency.

The day before IC-FPOP, 500 mL of a 125 mM quench solution containing 125 mM of PBN, 125 mM of DMTU, and 1% DMSO (added on the day of IC-FPOP) was made and solubilized in 500 mL Millipore water. The quench solution was mixed at 4°C. On the day of IC-FPOP experimentation, 8 µL of CellROX Deep Red (final concentration of 5 µM) was added to each well. The six-well plates were incubated for 30 minutes at 37°C. Afterwards, the media was removed, and the cells were rinsed thrice with PBS.

## **PIXY 2.0**

IC-FPOP utilizes a sterile incubation system containing a mobile stage for movement in the XY direction as well as peristaltic pumps featuring perfusion lines for chemical transport, and mirrors to focus and direct the laser beam. PIXY is partnered with software that provides automated communication between the pumping system and the laser to facilitate the execution of the entire system. The second-generation PIXY system has an ECHO revolve fluorescence microscope added (Figure 1). To accommodate movement of the stage top incubator for fluorescence imaging, an extended rail system was also added. After IC-FPOP of an individual well the stage top incubator is moved toward the microscope for fluorescence imaging. The laser light is irradiated downward onto an individual well of the plate. The rail system moves the incubator so that the next well is in the pathway of the laser irradiation.

While the PIXY automation was not functional during experimentation, samples were still handled in the incubator, using one of the pumps for H<sub>2</sub>O<sub>2</sub> and quench application. For irradiation of each well, the flow automation was instituted, and once one well's sample was



irradiated, the plate was manually transferred to the fluorescence microscope, where fluorescence imaging was conducted.

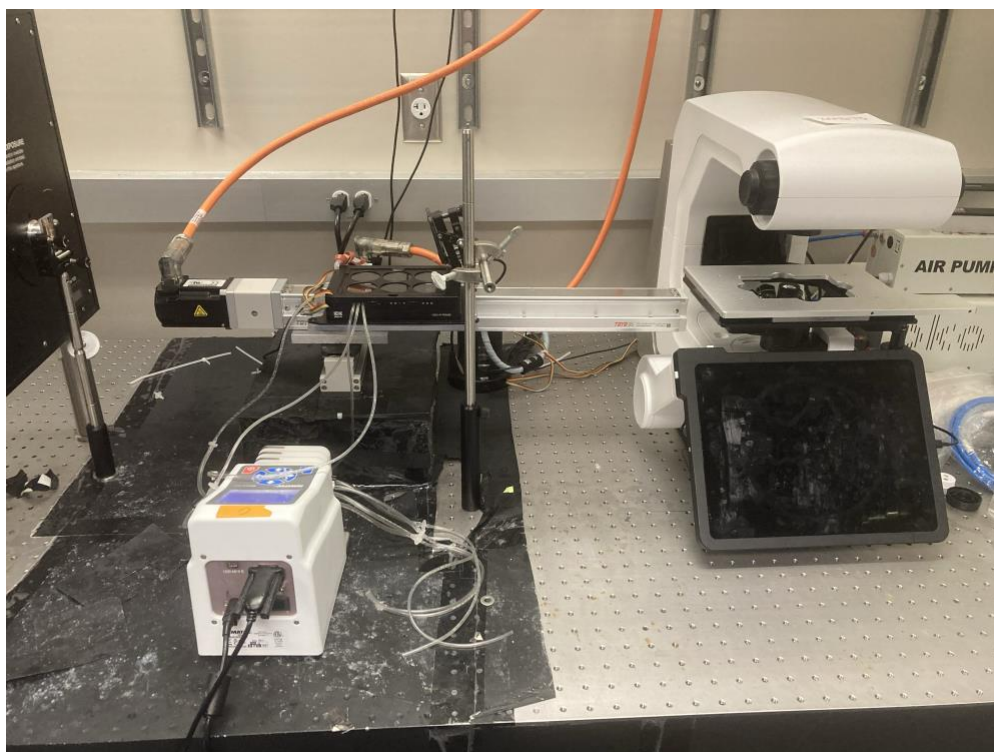


Figure 1: PIXY 2.0. The second-generation PIXY system has an ECHO revolve fluorescence microscope added. To accommodate movement of the stage top incubator for fluorescence imaging, there is also an extended rail system.<sup>3</sup> After IC-FPOP of an individual well the stage top incubator is moved toward the microscope for fluorescence imaging.

### **IC-FPOP to Test [H<sub>2</sub>O<sub>2</sub>] Gradient**

Five concentrations of H<sub>2</sub>O<sub>2</sub>—0mM, 20mM, 40mM, 80mM, and 100mM—were prepared in PBS. The 248 nm excimer laser was powered on and allowed to warm up. The PIXY Benchmark Script (Figure 2) was opened in LabVIEW, and the script was tested to ensure adequate liquid flow. Then, the quench solution and 0mM [H<sub>2</sub>O<sub>2</sub>] (i.e. PBS) were run until their respective lines were filled.

Once the laser was warmed up, the laser energy was tested using the Ophir Sensor at each of the mirrors and at the incubator's base where the sample would be. If the average laser energy

was not at least 120 mJ at the incubator's base, the laser gas was partially emptied and refilled. The laser energy was tested at each of the three locations after each gas refill. PIXY was then aligned by adjusting the rail system until the laser irradiated a single well of the six-well plate in its entirety. After laser alignment, the laser was set to 50 Hz, 26.00 kV, and to 1 pulse.

After being incubated with CellROX Deep Red for thirty minutes, removal of media, and three PBS rinses, the HEK293 cells were placed in the stage top incubator. Tubes primed with H<sub>2</sub>O<sub>2</sub> and the quench solution were fed into the sides of the stage top incubator. The fully automated script was initiated, and the laser fired immediately following the addition of the H<sub>2</sub>O<sub>2</sub>. IC-FPOP was conducted at each [H<sub>2</sub>O<sub>2</sub>] using the laser and without the laser (non-laser).

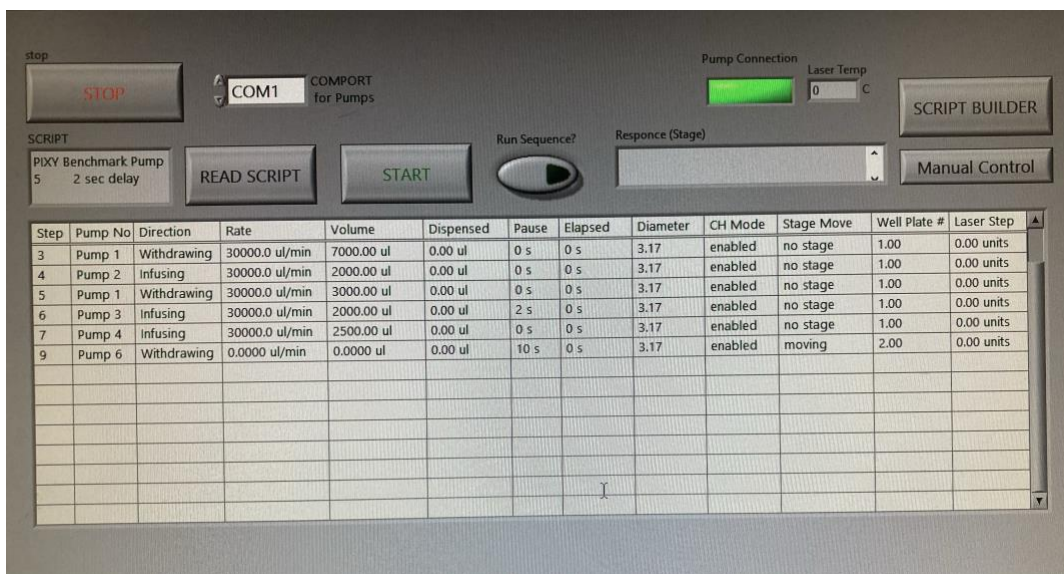


Figure 2: LabVIEW PIXY Benchmark script for a six-well plate.

### Fluorescence Imaging

Fluorescence imaging was conducted on the Echo Revolve fluorescence microscope directly following the addition of the quench solution. The microscope's objective was set to 1.25X|0.3, and sample protection (SP) was selected. The sample plate was placed on the microscope's dock and adjusted until focused on the well prepared for imaging. Transmitted

Light (TRANS) mode was selected for viewing of the sample under brightfield conditions to ensure the microscope lens was properly focused and that cells were still adhered to the well plate. ‘Levels’ was set to auto, so the microscope’s software automatically adjusted the brightness and contrast based on the image data being received. If images were out of focus, the necessary adjustments were made. Cy5 mode was then selected, and the sample was viewed. The imaging focus was again checked and adjusted. Once the image was as focused as possible, it was captured as .tiff (for image analysis) and jpeg files (for image viewing) and saved. Figure 3 demonstrates IC-FPOP workflow from coating collagen plates to fluorescence imaging.

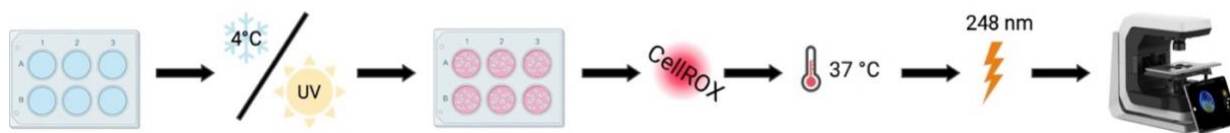


Figure 3: IC-FPOP Workflow.

## Results and Discussion

Baseline imaging of samples at 100 mM [H<sub>2</sub>O<sub>2</sub>] only were done to ensure sample fluorescence was successful. After this was confirmed, IC-FPOP and fluorescence imaging was done in triplicates for all five [H<sub>2</sub>O<sub>2</sub>] under laser and non-laser conditions. Initial fluorescence imaging showed that in some of the wells, cells had become detached from the collagen-coated well plate making clear imaging difficult. Image analysis was conducted on the Echo Revolve first, with the blurred images and then, a second time, removing the blurred images from the data pool. To determine the fluorescence intensity of sample images, the area of the image was selected on the Echo Revolve, producing the intensity output. The triplicate fluorescence intensities were averaged for each [H<sub>2</sub>O<sub>2</sub>] and graphed as mean fluorescence intensity (au) versus [H<sub>2</sub>O<sub>2</sub>] (mM). Predictably, the inclusion of the visibly blurred images resulted in no trend between fluorescence intensity and [H<sub>2</sub>O<sub>2</sub>]. However, when the blurred images were not

included, a trend became clear. Results showed that while there was an upward trend in fluorescence as the H<sub>2</sub>O<sub>2</sub> gradient increased, indicating successful oxidation and a linear response of CellROX Deep Red as a dosimeter in IC-FPOP, at 80 mM [H<sub>2</sub>O<sub>2</sub>] and higher, fluorescence was shown to have begun decreasing (Figure 4).

These results suggest that photobleaching, probe degradation, fluorescence quenching, sample degradation, probe diffusion, or another factor may have contributed to the declining mean fluorescence intensity after 40 mM [H<sub>2</sub>O<sub>2</sub>].

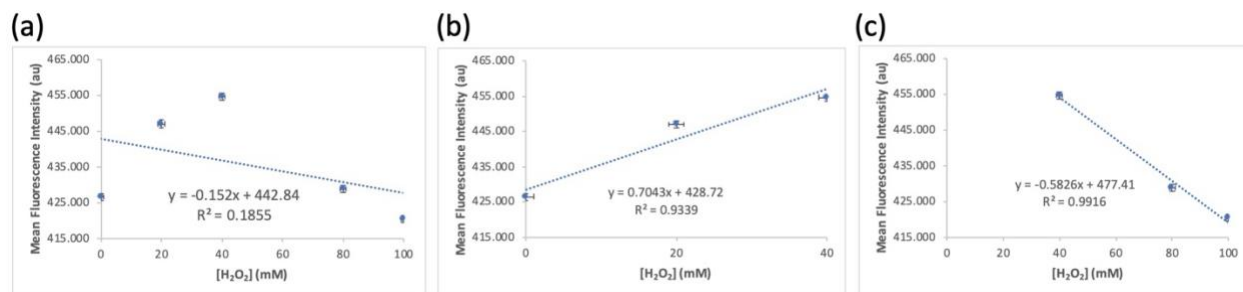


Figure 4: Dose response curve of CellROX Deep Red in laser samples at different concentrations of hydrogen peroxide (0, 20, 40, 80, and 100 mM). Fluorescence at 649-669 nm of 5 mM CellROX Deep Red with (a) different concentrations of hydrogen peroxide (0, 20, 40, 80, and 100 mM); different concentrations of hydrogen peroxide (0, 20, and 40mM) before fluorescence degradation; (c) different concentrations of hydrogen peroxide (40, 80, and 100 mM) after fluorescence degradation. Each data point is an average of two to three IC-FPOP oxidation replicates.

## Chapter 2 Troubleshooting and Optimization of Fluorescence Imaging

Fluorescence imaging under the previously outlined conditions proved insufficient. To address this, limitations of the fluorescence probe were taken into consideration. First, a method was sought out to improve the determination of mean fluorescence intensity. To improve fluorescence imaging analysis, different thresholds were assessed in ImageJ, a National Institute of Health (NIH) and Laboratory for Optical and Computational Instrumentation (LOCI) developed Java-based image processing program. Likewise, all experimentation was conducted in the dark to limit sample exposure to background light. The microscope's objective setting was changed to 10X|0.3 for clearer imaging. These changes were applied to a second group of trials.

Another concern was gaining better imaging coverage of wells, as the microscope being used only covered part of a single well. A more reliable, precise, and efficient method for determining the mean fluorescence intensity of an entire well was sought. This change as well as the changes from the previous paragraph were applied to a third group of trials.

### **Analysis in ImageJ: Testing Different Thresholds**

An adjustment that was made was in the manner in which mean fluorescence intensity was calculated. Previously, the Jones lab manually determined the mean fluorescence intensity by focusing on three sections of cells in a well and averaging their intensities on the Echo.<sup>2</sup> However, an ImageJ protocol was developed to better analyze fluorescence images using thresholds.

Thresholds are computational methods used to transform a greyscale image into a binary image for analysis. Thresholds are necessary because fluorescence images typically have regions of varying intensity levels, and thresholding helps isolate regions the regions where intensity exceeds a certain level, focusing on fluorescently labeled areas relevant to analysis. Thresholding

also helps to reduce background fluorescence, reducing noise. All sixteen available thresholds were attempted on the first of the .tiff images to gauge which auto threshold demonstrated visible areas of fluorescence comparable to the jpeg image. The most comparable threshold for the first 0mM [H<sub>2</sub>O<sub>2</sub>] trial was Triangle. However, this proved to be an ineffective method, as the optimal threshold changed from image to image due to variability in lighting and focus of each of the captured images. Therefore, a manual thresholding method was adopted.

### Image J Protocol Using Manual Thresholding

The most recent version of ImageJ (ImageJ 1.53t) was downloaded and opened. The applicable measurements were selected ("Analyze" => "Set Measurements) as "Area," "Standard deviation," "Min & max gray value," "Mean gray value," and "Display label" (Figure 6). "Redirect to:" was set at "None," and the number of decimal places was set to three. "OK" was pressed to set the selected measurements.

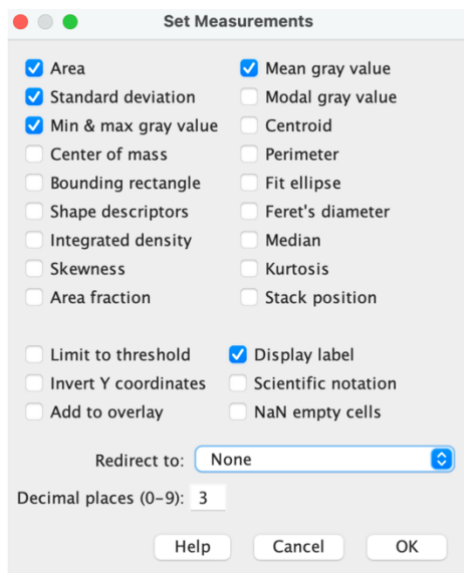


Figure 5: ImageJ Set Measurements.

To begin fluorescence imaging analysis, the first .tiff sample file was opened in ImageJ ("File" => "Open" => Select .tiff file). An auto threshold method was applied to the .tiff image

(“Image” => “Adjust” => “Threshold,”) bringing up a histogram and threshold settings (Figure 7). The auto-threshold method was disregarded, as thresholding was done manually. The display mode was set to “Red.” “Dark background” and “Don’t reset range” were selected. Using the slider directly below the histogram, the threshold range was adjusted to exclude everything but the right-most tail end of the peak; everything within the red rectangle was included in the threshold range. The manually adjusted image was compared to the jpeg image to ensure the image matched the fluorescence visible in the jpeg, after which the threshold was set by pressing “Apply.” Mean fluorescence intensity was measured (“Analyze” => “Measure.”) This was done for all .tiff images.

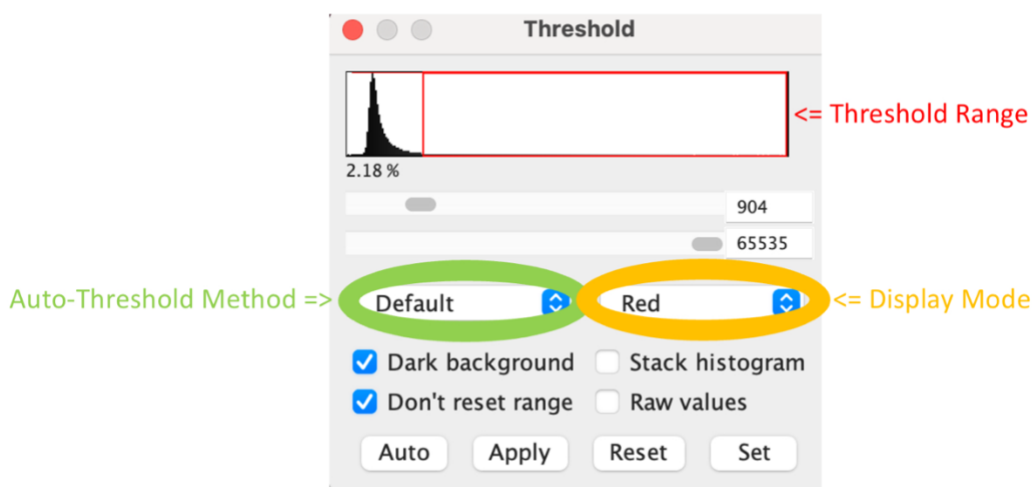


Figure 6: Manual Thresholding in ImageJ.

### IC-FPOP Using A 24-Well Plate

Twenty-four-well collagen plates were used to ensure better fluorescence imaging coverage. At this smaller size, the imaging scope was able to cover the entirety of a single well, rather than just a part of it. The LabVIEW script was likewise modified to accommodate a twenty-four well-plate (Figure 5), with adjusted volumes to match the target concentrations outlined in the above chapter.



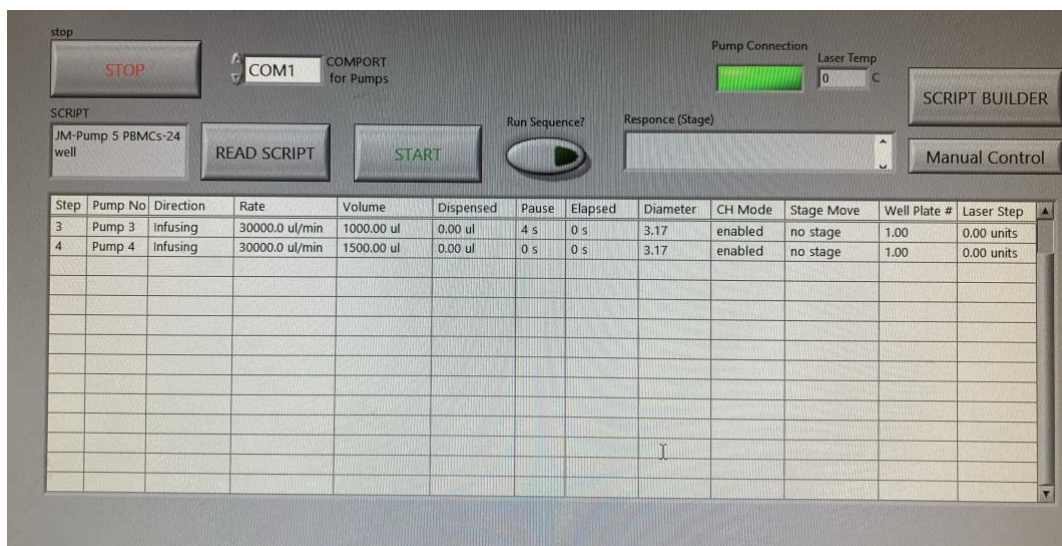


Figure 7: LabVIEW 24-well automated script.

## Data and Results

Manual thresholding of the trials was completed for the second group of trials, which was done in a six-well plate. The results showed a linear response, where, as the concentration of  $\text{H}_2\text{O}_2$  increased, so did the mean fluorescence intensity through 80 mM  $[\text{H}_2\text{O}_2]$  (Figure 8). However, there was a decrease in mean fluorescence intensity from 80 mM to 100 mM  $[\text{H}_2\text{O}_2]$ , indicating fluorescence degradation.

Results for the trials in the 24-well plate using manual thresholding resulted in a linear response (Figure 9), demonstrating a positive correlation between mean fluorescence intensity and  $[\text{H}_2\text{O}_2]$ . However, it should be noted that only two trials were completed for each concentration of hydrogen peroxide.



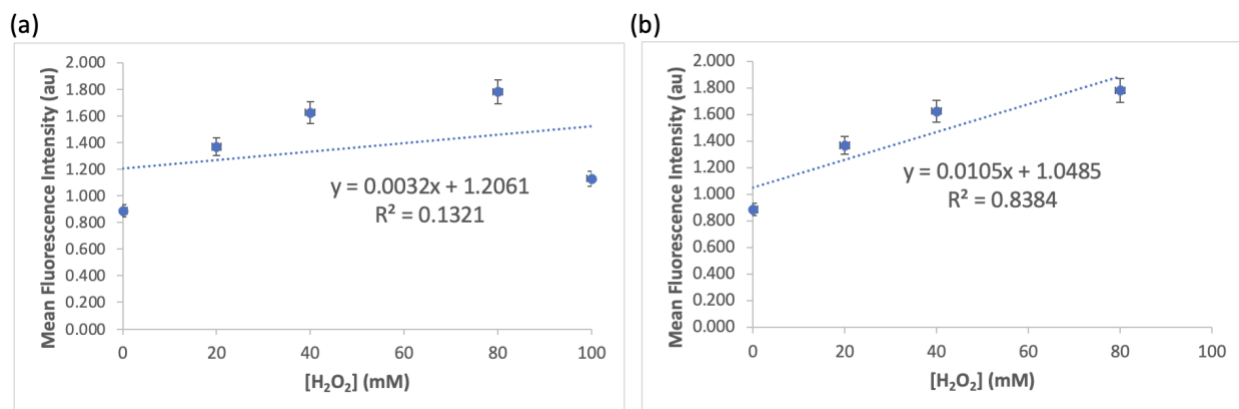


Figure 8: Dose response curve of CellROX Deep Red in laser samples at different concentrations of hydrogen peroxide (0, 20, 40, 80, and 100 mM) after manual thresholding in ImageJ. Fluorescence at 649-669 nm of 5 mM CellROX Deep Red with (a) different concentrations of hydrogen peroxide (0, 20, 40, 80, and 100 mM); different concentrations of hydrogen peroxide (0, 20, 40, and 80 mM) before fluorescence degradation. Each data point is an average of three IC-FPOP oxidation replicates.

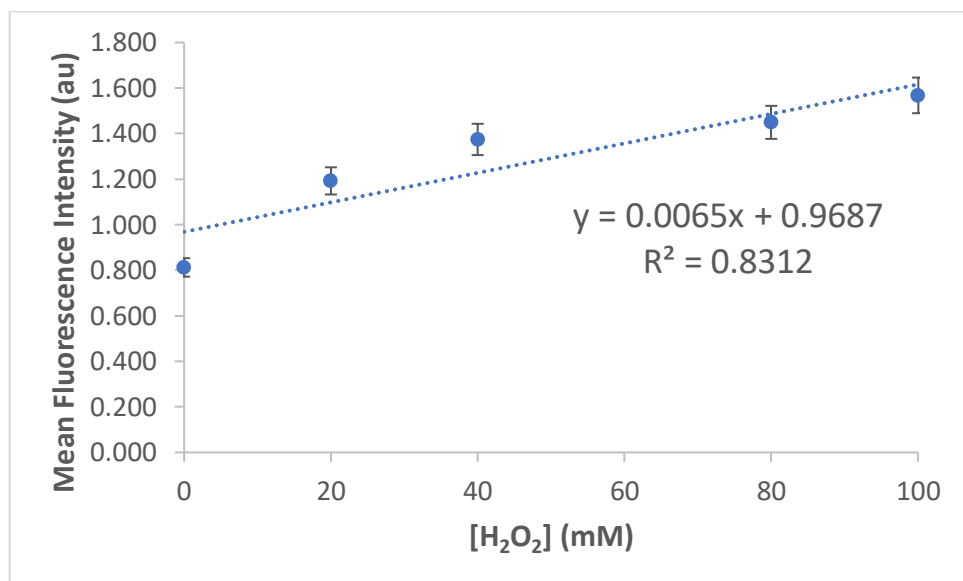


Figure 9: Dose response curve of CellROX Deep Red in 24-well plate laser samples at different concentrations of hydrogen peroxide (0, 20, 40, 80, and 100 mM) after manual thresholding in ImageJ. Fluorescence at 649-669 nm of 5 mM CellROX Deep Red with different concentrations of hydrogen peroxide (0, 20, 40, 80, and 100 mM). Each data point is an average of two IC-FPOP oxidation replicates.

## **Potential Pitfalls/Alternative Directions**

The time it takes to manually complete the IC-FPOP workflow may have had an impact on the results of laser versus non-laser samples. The amount of time CellROX Deep Red was in contact with the sample may have affected the intensity reading. As IC-FPOP on the laser samples was done last, this may be why by the time they underwent IC-FPOP (more than an hour after incubation), the signal had begun to fade, resulting in a lower fluorescence intensity in some samples. On the other hand, fluorescence in the non-laser samples may have been observed as a result of background oxidation. Fixing the PIXY automation should become next priority to reduce time as a factor and make the IC-FPOP process more precise and efficient.

It was further noted that manual thresholding often introduces bias to fluorescence imaging analysis. To account for this, manual thresholding was compared to the visible fluorescence in the jpeg image. Also, mean fluorescence intensity measurements weren't viewed until after all the samples had been thresholded. Despite this, a more unbiased and efficient method should be determined for future ImageJ fluorescence imaging.

## CONCLUSION

Although a linear response of the radical dosimeter CellROX Deep Red was not definitively established, results proved positive, showing an upward trend in oxidation to a certain extent. While increasing  $\text{H}_2\text{O}_2$  concentration did not result in increased fluorescence intensity in all samples as expected, there was a correlation in the six-well plate trials, as evidence by increasing fluorescence below 80 mM after excluding outliers (due to grainy or blurred imaging) for the first set of trials and 100 mM in the second set. However, above 60 mM  $[\text{H}_2\text{O}_2]$  and 80 mM respectively, fluorescence intensity began to decline. The reason behind this decrease may have been due to photobleaching, probe degradation, fluorescence quenching, sample degradation, probe diffusion, or a number of other reasons. More experimentation is needed to draw further conclusions.

### **Potential Pitfalls/Alternative Directions**

Should CellROX Deep Red not present a linear relationship with fluorescence intensity, other fluorescence probes such as hydroxyphenyl fluorescein (HPF), 2-(6-(4'-amino) phenoxy-3H-xanthen-2-on-9-yl) benzoic acid (APF), or 5,5-dimethyl-1-pyrroline N-oxide (DMPO), which fluoresce only in the presence of hydroxyl radicals, may be used. These probes are already accessible in the lab and are promising alternatives should CellROX Deep Red prove non-linear.

An alternative method to address the time it takes to conduct fluorescence imaging and the effect this has on the fluorescence probe would be to introduce a fixative to samples (i.e. formaldehyde). Adding a fixative such as formaldehyde would increase the length of time before degradation of the fluorophore to provide more time to take focused fluorescence images.

## Future Directions

Several trials at 0 mM only should be done to determine the best fluorescence imaging settings for minimal fluorescence. This was conducted for 100 mM to confirm a fluorescent response. However, after optimal fluorescence imaging settings are determined from the 0 mM trials, another set of 100 mM trials should be conducted to ensure fluorescence is still observed under the new settings.

Once a linear response is established, the effect of laser energy and DMSO on effective radical dose should be tested in order to optimize the conditions for HRPF experiments (Table 1). It is expected that there will be a positive correlation between mean fluorescence intensity and laser energy, whereas for mean fluorescence intensity and DMSO, there will be a negative correlation, as DMSO is a radical scavenger.

Table 1: Experimental outline with predicted outcomes. A) [H<sub>2</sub>O<sub>2</sub>] gradient: B) Laser Energy gradient: C) DMSO gradient:

Condition	[H <sub>2</sub> O <sub>2</sub> ] (mM)	Laser Energy (mJ)	DMSO (mM)	Predicted Outcome
<b>A</b>	0-150	110	0	Directly Proportional
<b>B</b>	100	Gradient (40-160)	0	Directly Proportional
<b>C</b>	100	110	0-0.5%	Indirectly Proportional
<b>Control</b>	100	0	0	N/A

## REFERENCES

- (1) Abaandou, L.; Quan, D.; Shiloach, J. Affecting HEK293 Cell Growth and Production Performance by Modifying the Expression of Specific Genes. *Cells* 2021, 10, 1667. <https://doi.org/10.3390/cells10071667>
- (2) Johnson, D. T. (2022) *Method Optimization of a New Automated Platform for Proteome-Wide Structural Biology*. University of Maryland Baltimore, Doctor of Philosophy. <http://hdl.handle.net/10713/20364>
- (3) Johnson, D. T., Punshon-Smith, B., Espino, J. A., Gershenson, A., & Jones, L. M. (2020). Implementing In-Cell Fast Photochemical Oxidation of Proteins in a Platform Incubator with a Movable XY Stage. *Analytical chemistry*, 92(2), 1691–1696. <https://doi.org/10.1021/acs.analchem.9b04933>
- (4) Kaur, U., Johnson, D. T., & Jones, L. M. (2020). Validation of the Applicability of In-Cell Fast Photochemical Oxidation of Proteins across Multiple Eukaryotic Cell Lines. *Journal of the American Society for Mass Spectrometry*, 31(7), 1372–1379. <https://doi.org/10.1021/jasms.0c00014>
- (5) Misra, S. K., Orlando, R., Weinberger, S. R., & Sharp, J. S. (2019). Compensated Hydroxyl Radical Protein Footprinting Measures Buffer and Excipient Effects on Conformation and Aggregation in an Adalimumab Biosimilar. *The AAPS journal*, 21(5), 87. <https://doi.org/10.1208/s12248-019-0358-2>
- (6) Pulix, M., Lukashchuk, V., Smith, D. C., & Dickson, A. J. (2021). Molecular characterization of HEK293 cells as emerging versatile cell factories. *Current opinion in biotechnology*, 71, 18–24. <https://doi.org/10.1016/j.copbio.2021.05.001>
- (7) Sharp, J. S., Misra, S. K., Persoff, J. J., Egan, R. W., & Weinberger, S. R. (2018). Real Time Normalization of Fast Photochemical Oxidation of Proteins Experiments by Inline Adenine Radical Dosimetry. *Analytical chemistry*, 90(21), 12625–12630. <https://doi.org/10.1021/acs.analchem.8b02787>
- (8) Xie, B., & Sharp, J. S. (2015). Hydroxyl Radical Dosimetry for High Flux Hydroxyl Radical Protein Footprinting Applications Using a Simple Optical Detection Method. *Analytical chemistry*, 87(21), 10719–10723. <https://doi.org/10.1021/acs.analchem.5b02865>